

Preparation of topoisomers of short circular dsDNA with defined linking number by accurate topological control

Mengqin Liu^{1,*}, Ziyi Wang^{1,†}, Ran An^{1,2,*}, Angda Li¹, Xingguo Liang^{1,2,*}

¹State Key Laboratory of Marine Food Processing and Safety Control, College of Food Science and Engineering, Ocean University of China, Qingdao 266404, China

²Laboratory for Marine Drugs and Bioproducts, Qingdao Marine Science and Technology Center, Qingdao 266237, China

*To whom correspondence should be addressed. Email: liumengqin831@ouc.edu.cn

Correspondence may also be addressed to Ran An. Email: ar@ouc.edu.cn

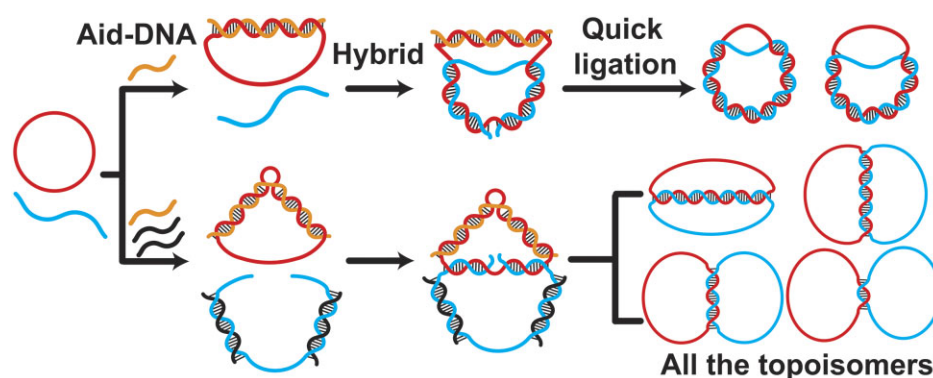
Correspondence may also be addressed to Xingguo Liang. Email: liangxg@ouc.edu.cn

[†]The first two authors should be regarded as Joint First Authors.

Abstract

Short DNA catenanes [circular double-stranded DNA (dsDNA)] have attracted considerable interest for constructing nanostructures and nanomachines, as well as understanding DNA topology. The study of topoisomers of a circular dsDNA with a definite linking number (Lk) is essential but very difficult for simplifying the complex problems about DNA topology. The topoisomers are difficult to prepare, especially in the case that two strands are completely complementary. In this study, using a model system, we prepared all eight topoisomers (Lk0–Lk7) of a 79-bp-long circular dsDNA (8–14 nm in size) by utilizing aid-DNA to prevent undesired hybridization. By rapid ligation before strand displacement, high selectivity (>75%) for most topoisomers (31% for Lk1) was achieved under the strict topological control. All eight topoisomers with high purity were obtained after purification. Using a gel shift assay with Z-DNA-specific binding proteins, as well as by circular dichroism chromatography and enzymatic digestion, it was found that Z-DNA forms for topoisomers Lk0–Lk6, and Lk0–Lk5 can be converted to Lk6 by topoisomerase I. The approach developed in this study can significantly contribute to DNA or RNA topology, particularly the effect of topological constraints on DNA structures and functions.

Graphical abstract



Introduction

DNA topology is of great significance to biology, but the corresponding mechanisms are still unclear. It is well known that the circular double-stranded DNA (dsDNA) genome of a plasmid or bacterium is a catenane of two complementary single-stranded DNAs (ssDNA), wherein these two strands wind (or intertwine around each other) for many turns (~10.4 bp/turn). Notably, a segment (ranging from hundreds to thousands of base pairs) of the linear genome in eukaryotic cells exhibits a similar topology to that of circular dsDNAs, given

the immense size of chromosomes (usually longer than 10^7 bp) (Supplementary Fig. S1). The regulation of this DNA topology is of great significance for biological systems. In *Escherichia coli*, for example, the topoisomerases can modulate supercoiling to an optimal density (approximately –10% to –5%). The superhelical density (σ), also referred to as “specific linking difference,” equals $(Lk - Lk_0)/Lk_0$, where Lk is the actual linking number of a circular dsDNA and Lk_0 is the number of turns in the relaxed DNA. Negatively supercoiled DNA has relatively high free energy and tends to unwind the DNA

Received: October 22, 2024. Revised: April 10, 2025. Editorial Decision: April 18, 2025. Accepted: May 16, 2025

© The Author(s) 2025. Published by Oxford University Press on behalf of Nucleic Acids Research.

This is an Open Access article distributed under the terms of the Creative Commons Attribution-NonCommercial License

(https://creativecommons.org/licenses/by-nc/4.0/), which permits non-commercial re-use, distribution, and reproduction in any medium, provided the original work is properly cited. For commercial re-use, please contact reprints@oup.com for reprints and translation rights for reprints. All other permissions can be obtained through our RightsLink service via the Permissions link on the article page on our site—for further information please contact journals.permissions@oup.com.

double helix, which facilitates replication and transcription [1–3]. Due to this torsional stress for unwinding (or unwinding stress), other DNA secondary structures prefer to form, such as Z-DNA [4–6], cruciform DNA structures [3, 7], and triple helix (H-DNA) [8, 9], which can play roles in gene regulation. Obviously, the dsDNA circles with the same sequence but varying linking numbers (referred to as DNA topoisomers) are essential materials for the study of DNA topology. However, it is very difficult to precisely control the topology of circular dsDNA to achieve a specific and desired state, especially when two ssDNA strands are completely complementary.

It has been reported that the formation of Z-DNA can play a role in gene regulation associated with cancer cell metastasis, oxidative tissue damage, necroptosis, and inflammation [10–14]. Endogenous Z-DNA binding proteins in humans, such as ZBP1 (an innate immune sensor) and ADAR1 (double-stranded RNA-specific adenosine deaminase), have significant functions in these processes [12, 13]. Nevertheless, we are still far from understanding Z-DNA and these proteins. It has been found that Z-DNA can form almost for any sequence [not limited to alternating purine–pyrimidine (APP) sequences like (dCdG)_n] under the topological constraint of negative supercoils [15], suggesting that Z-DNA (as well as Z-RNA) is much easier to form than we thought. The left-handed structure may play a persistent role in normal cells. Therefore, there is an urgent need for accessible tools and materials to study DNA topology and Z-DNA. However, traditional models that generate topological stress and induce DNA unwinding, such as plasmids and nucleosomes, face challenges in precisely controlling a short Z-DNA (~12 bp) or a transcription bubble (~17 bp). In contrast to long dsDNA molecules, the short circular dsDNAs (30–150 bp), which cannot form negative supercoils due to the rigidity of dsDNA, have the potential to simulate the unwinding of DNA duplexes.

Several studies have attempted to unravel the mysteries of DNA topology [15–33]. For example, mixtures of multiple topoisomers with negative supercoils ($|\sigma| < 17\%$) of circular plasmid dsDNA (>2000 bp) were prepared using ethidium bromide (EB) as the intercalator: a relaxed plasmid with a nick was first mixed with EB, followed by ligation with T4 DNA ligase [16–19]. Similarly, DNA minicircles ranging from 454 to 235 bp with higher superhelical density ($|\sigma| < 27\%$) were successfully generated [20–26]. However, precise control over the linking number remains challenging, and most topoisomers exist as mixtures [20, 27–29]. Furthermore, studying the topological effects is complicated due to the dynamic equilibrium between a supercoil state and the partially unwound state (Supplementary Fig. S1A) for a long circular dsDNA (>300 bp) [30, 31]. Bates and Hobson *et al.* reported that DNA minicircles (116 bp) exhibited a superhelical density close to -20% after treatment with DNA gyrase [27, 32], but obtaining other isomers proved difficult. It is well established that DNA minicircles shorter than 150 bp struggle to form supercoils due to the rigidity of dsDNA. We showed that a short (70–111 bp) circular dsDNA (Lk = 0) forms the Z–B chimera (consisting of a Z-DNA segment and a B-form segment) without forming supercoils [15, 33]. In a nucleosome, 146-bp dsDNA wraps around the histone complex in 1.65 turns (88.5 bp/turn, $\sigma = -11.8\%$) to form the negative supercoil of toroid style, i.e. one-start left-handed helix, which is different from the plectoneme style (two-start right-handed helix with terminal loops). If the histones dissociate, a loop structure of ~200 bp is formed with topological stress

($\sigma = -8.6\%$). Accordingly, constructing topoisomers of dsDNA minicircles (<100 bp) may provide deeper insights into DNA topology and its biological significance.

Several groups have attempted to prepare topoisomers of small ssDNA catenanes. Li *et al.* reported that two topological isomers (Lk1 and Lk2) shorter than 100 nt could be obtained for a catenane formed from two ssDNAs that are partially complementary to each other [34]. It is noteworthy that, in this study, Lkn ($n = 0–7$) denotes the topoisomer with a linking number of n (e.g. Lk5 indicates the topoisomer with a linking number of 5). They employed scaffold DNAs to prevent undesired hybridization, especially for preparing the catenane of Lk1 (the topoisomer with a linking number of 1). However, these topoisomers are less biologically significant because they contain dozens of mismatches (with high flexibility), making it difficult to induce topological constraint. Thomas *et al.* prepared a mixture of topoisomers of Lk7 and Lk8 for a 95-bp circular dsDNA ($\Delta\text{Lk} = -2$ and -1 , corresponding to superhelical densities of -11% and -22% , respectively) using EB [35]. Du *et al.* obtained the specific topoisomers of 84-bp ($\Delta\text{Lk} = -1$, $\sigma = -12.5\%$) and 63-bp catenane ($\Delta\text{Lk} = -1$, $\sigma = -16.7\%$) by controlling the ligation temperature [36]. However, these methods are unable to produce pure topoisomers with other linking numbers for further study.

Materials and methods

Materials

All oligonucleotides used in this study (see sequences in Supplementary Table S1) were purchased from Sangon Biotech (Shanghai, China). T4 polynucleotide kinase, T4 DNA ligase, exonuclease I, exonuclease III, ATP, UTP, GTP, CTP, RNase inhibitor, and DNA ladders were obtained from Thermo Scientific (Pittsburgh, PA, USA). Topoisomerase I (Topo-I), T7 RNA polymerase, *Hinf*I, *Bts*CI, *Eco*RI, BAL 31, and S1 nuclease were from New England Biolabs Inc. (Ipswich, MA, USA). BAL31 nuclease was from Takara Bio Inc. (Beijing, China). Z-DNA-specific antibody (Z22) was from Absolute Antibody Ltd (Oxford, UK). The fluorescent dye EvaGreen was from Biotium (Fremont, CA, USA), and Ultra GelRed (a dye that stains both dsDNA and ssDNA) was from Vazyme (Nanjing, China). All other chemicals were from Sigma–Aldrich (St. Louis, MO, USA).

Synthesis of circular ssDNA and linear DNA from two fragments by ligation

Prior to the ligation experiments, a phosphate group was enzymatically introduced to the 5'-end of each linear DNA substrate (La-p1, La-p2, Ls-p1, and Ls-p2). The solution for phosphorylation (40 μl) contained DNA substrate (40 μM), ATP (1.0 mM), and T4 polynucleotide kinase (0.625 U/ μl) in 1 \times buffer (50 mM Tris–HCl, 10 mM MgCl₂, 5.0 mM DTT, and 0.10 mM spermidine) and was incubated at 37°C for 12 h. The mixture was incubated at 75°C for 10 min. The preparation of circular DNA (Cs and Ca) was carried out using the one-pot ligation method from multiple fragments [37]. Single-stranded linear DNA substrates (final concentration of 2.0 μM), splints (final concentration of 4.0 μM), and T4 DNA ligase (final concentration of 0.10 U/ μl) were mixed in 100 μl of 0.1 \times T4 DNA ligase buffer (0.05 mM ATP, 1.0 mM MgCl₂, 1.0 mM DTT, and 4.0 mM Tris–HCl, pH 7.8 at 25°C). The reaction was incubated at 25°C for 12 h, and then terminated by incubating the mixture at 65°C for 10 min. For purification of the

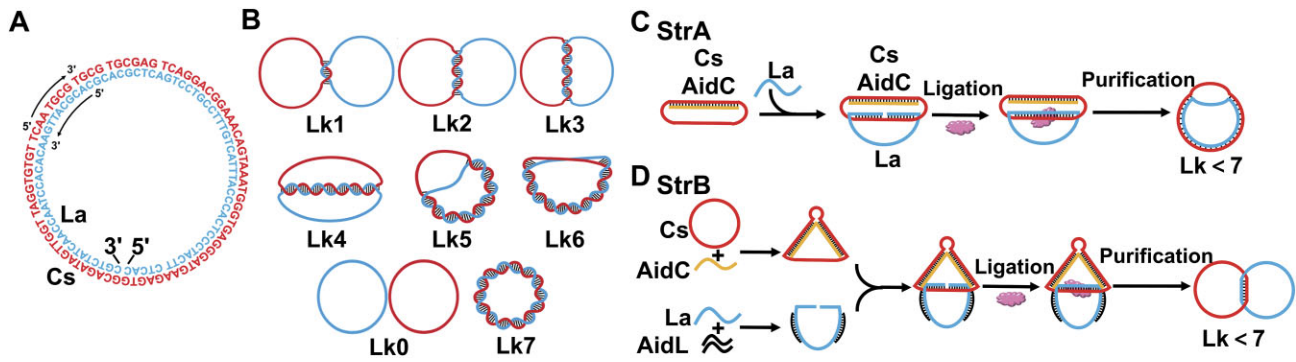


Figure 1. Strategy for preparing varying topoisomers (Lk0–Lk7) of a 79-bp-long dsDNA minicircle using topological control. **(A)** Sequences of Cs (circular DNA of the sense strand) and La (linear DNA of the antisense strand). **(B)** Structural diagram of each topoisomer with a specific Lk. **(C)** Schematic illustration of Strategy A (StrA). After AidC (aid-DNA complementary to the circular strand) hybridizes with Cs, La is added and immediately ligated by T4 DNA ligase. The aid-DNA prevents further hybridization between La and Cs, enabling the isolation of topoisomers (Lk4–Lk6). **(D)** Schematic illustration of Strategy B (StrB). AidC and AidL (aid-DNA complementary to the linear strand) are used. AidC hybridizes first with Cs to form a structure containing a 5-nt loop, facilitating the bending of the resulting duplex. Two AidL strands hybridize with La to inhibit strand displacement prior to ligation. By adjusting the length of AidC and AidL, varying topoisomers (Lk1–Lk4) with smaller linking numbers can be obtained. The lengths and complementary positions of aid-DNA strands are designed to control the Lk precisely (see sequences in [Supplementary Table S1](#)).

circular DNA (Cs and Ca), unreacted or by-products of linear DNA were removed by treatment with 1.0 U/μl exonuclease I in its 0.5× buffer (37.5 mM glycine–KOH, 3.35 mM MgCl₂, 5.0 mM β-ME, pH 9.5 at 25°C) at 37°C for 12 h [37].

Preparation of topoisomers of short circular dsDNA using Strategy A

The basic procedure for StrA (Fig. 1C): After mixing Cs and AidC in a buffer, the solution was heated to 90°C and maintained for 3 min. The solution was gradually cooled (0.1°C/s) from 90°C to 25°C and incubated at 25°C for 10 min. T4 DNA ligase was added first to above solution, and then La was added and incubated at 25°C for 30 min. The reaction was terminated by incubating at 65°C for 10 min (inactivation of T4 DNA ligase), followed by treatment with exonuclease I and exonuclease III at 37°C for 2 h to digest any remaining linear DNAs. For polyacrylamide gel electrophoresis (PAGE) analysis, 0.5 pmol of DNA samples were typically loaded.

Typical conditions for ligation (20 μl total volume; see Fig. 2 and [Supplementary Table S1](#) for sequences): 2.4 μl of prepared Cs (1.7 μM in 0.5× exonuclease I buffer, 0.08× T4 DNA ligase buffer, and 0.08× T4 polynucleotide kinase buffer), 0.8 μl of La (5.0 μM in 1.0× T4 DNA ligase buffer), 2.0 μl of AidC (2.4 μM in H₂O), 2.0 μl of T4 DNA ligase buffer (10×), and 11.8 μl of H₂O were added. Then, 1 μl of T4 DNA ligase (1 U/μl) and 0.8 μl of La (5 μM in 1× T4 DNA ligase buffer) were added. The final concentrations of Cs, La, AidC, and ligase were 0.2 μM, 0.2 μM, 0.24 μM, and 50 U/ml, respectively.

Typical protocol and conditions for digestion by exonucleases (21.6 μl total volume): To 20 μl of the above solution, 0.8 μl of exonuclease I (10 U/μl) and 0.8 μl of exonuclease III (5.0 U/μl) were added. The final concentrations of exonuclease I and exonuclease III were 0.37 and 0.19 U/μl, respectively.

Preparation of topoisomers of circular dsDNA using StrB

The basic procedure for StrB (Fig. 1D): After mixing Cs and AidC in a buffer, the solution was heated to 90°C and main-

tained for 3 min. The solution was gradually cooled (0.1°C/s) from 90°C to 25°C, and incubated at 25°C for 10 min to obtain Mix-A. Similarly, Mix-B containing La and AidL was prepared according to above protocol. After T4 DNA ligase was added to Mix-A, Mix-B was added, and then incubated at 25°C for 30 min. The reaction was terminated and treated with exonuclease I and exonuclease III with the similar protocol as StrA.

Typical conditions for ligation (20 μl total volume): For Mix-A, 2.4 μl of Cs (1.7 μM in 0.5× exonuclease I buffer, 0.08× T4 DNA ligase buffer, and 0.08× T4 polynucleotide kinase buffer), 2.0 μl of AidC (2.4 μM in H₂O), 1.0 μl of T4 DNA ligase buffer (10×), and 4.6 μl of H₂O were mixed. For Mix-B, 0.8 μl of La (5 μM in 1× T4 DNA ligase buffer), 2.0 μl of AidL^a (2.4 μM in H₂O), 2.0 μl of AidL^b (2.4 μM in H₂O), 1.0 μl of T4 DNA ligase buffer (10×), and 2.2 μl of H₂O were mixed. After 2 μl of T4 DNA ligase (1.0 U/μl) was added to Mix-A, Mix-B was added. The final concentrations of Cs, La, AidC, AidL, and ligase were 0.2 μM, 0.2 μM, 0.24 μM, 0.24 μM, and 0.1 U/μl, respectively.

Preparation of the topoisomer Lk1 using a long linear phosphorothioated aid-DNA (first circularized and then linearized using I₂)

To a tube, 4.8 μl of Cs (1.7 μM), 1.6 μl of AidC104 (6 μM), and 1.0 μl of T4 DNA ligase buffer (10×) were mixed. The mixture was heated to 90°C and kept for 3 min, and it was gradually cooled (0.1°C/s) to 25°C and kept for 10 min. Then, 1.0 μl of T4 DNA ligase (5.0 U/μl) and 1.6 μl of La were added, followed by incubation at 25°C for 30 min for ligation. To above solution (10 μl), 1.6 μl of Splint a_{1-p2}, 1.0 μl of T4 DNA ligase buffer (10×), 1.0 μl of T4 DNA ligase (5.0 U/μl), and 6.4 μl of water were added, followed by incubation at 25°C for 30 min for ligation, subsequently increased to 65°C for 10 min (inactivate the ligase).

To the above mixture (20 μl), 4.0 μl of I₂/KI solution (30 mM I₂, 150 mM KI), 4 μl of Tris–HCl buffer (pH 9.0, 500 mM), and 12 μl of water were added and incubated at 25°C for 60 min [38]. Finally, the solution was treated with 1.0 U/μl exonuclease I and 1.0 U/μl exonuclease III with the similar protocol as described previously.

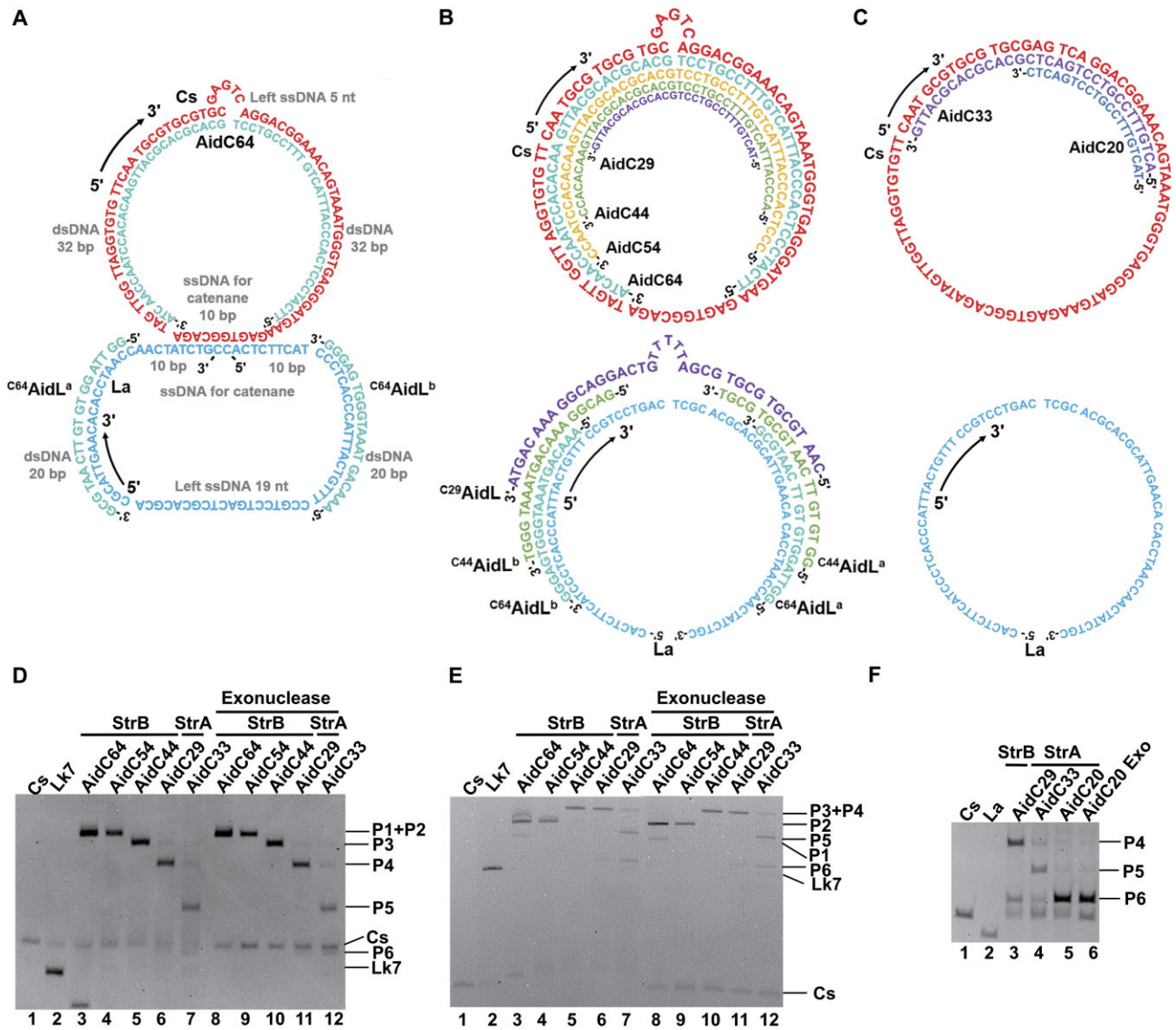


Figure 2. Sequence design (A, B, C) and dPAGE analysis of ligation results (D, E, F) for preparing six topoisomers. (A) For preparing Lk1 using one AidC for protecting Cs and two aid-DNAs for La. The nomenclature: AidC64 indicates it is 64 nt long and complementary to Cs; ^{C64}AidL^a works together with AidC64 to prepare a topoisomer. (B) For preparing Lk1, Lk2, Lk3, and Lk4 (StrB). ^{C64}AidL^a and ^{C64}AidL^b work together with AidC64 (to prepare Lk1) or AidC54 (to prepare Lk2), ^{C44}AidL^a and ^{C44}AidL^b with AidC44 to prepare Lk3, and ^{C29}AidL^a and ^{C29}AidL^b with AidC44 to prepare Lk4. (C) For preparing Lk5 and Lk6 (StrA). Aid-DNA for targeting La is not required. Panels (D) and (E) show 6% and 15% dPAGE results for analyzing the cases using AidC64, AidC54, AidC44, and AidC29 (StrB), as well as AidC33 (StrA). Lane 1: Cs; lane 2: Lk7 topoisomer obtained by ligating hybrid of Cs and Ls without protection by aid-DNAs; lanes 3–6: AidC64, AidC54, AidC44, and AidC29 (StrB); lane 7: AidC33 (StrA); lanes 8–12: digestion of products in lanes 3–7 by exonucleases. (F) Six percent dPAGE results for analyzing the cases using AidC29 (StrB) and AidC33 (StrA). Lane 1: Cs; lane 2: La; lane 3: AidC29 (StrB); lanes 4 and 5: AidC33 and AidC20 (StrA); lane 6: digestion of products in lane 5 by exonucleases. Cs and AidC, and La and AidL were hybridized in 1 × T4 DNA ligase buffer and 10 mM MgCl₂, followed by ligation by 0.40 U/μl T4 DNA ligase at 25°C for 30 min. [Cs] = [La] = 0.20 μM, [AidC] = [AidL] = 0.24 μM. dPAGE gel contains 25% formamide and 7.0 M urea.

Preparation of the topoisomer Lk5 using an aid-DNA that is circularized on Cs followed by linearized using *EcoRI*

To a tube, 1.6 μl of AidC69 (a linear ssDNA, 5.0 μM), 1.6 μl of ^{C69}AidA (partially complementary to AidC69, 6.0 μM), and 1.0 μl of 10× T4 DNA ligase buffer were mixed and annealed (90°C for 3 min, 0.1°C/s to 25°C, 25°C for 10 min). Then, 4.8 μl of Cs (1.7 μM) was added to the above mixture (4.2 μl) and incubated at 25°C for 10 min. After adding 1.0 μl of T4 DNA ligase (5.0 U/μl), the mixture (designated as Mix-A) was incubated at 25°C for 30 min. In another tube, 1.6 μl of La (5.0 μM), 1.0 μl of 10× T4 DNA ligase buffer,

and 6.4 μl ^{C69}AidL (1.5 μM) were added and annealed (90°C for 3 min, 0.1°C/s to 25°C, 25°C for 10 min) to obtain a mixture (designated as Mix-B). After 1.0 μl of T4 DNA ligase (5.0 U/μl) was added to Mix-A, Mix-B was added, and then incubated at 25°C for 30 min, and then 65°C for 10 min. The final concentrations of Cs, La, AidC69, ^{C69}AidA, ^{C69}AidL, and ligase were 0.4 μM, 0.4 μM, 0.4 μM, 0.48 μM, 0.48 μM, and 0.5 U/μl, respectively. Then, to the above mixture (20 μl), 4.0 μl of *EcoRI* (20 U/μl), 4.0 μl of 10× rCutSmart buffer [500 mM KAc, 200 mM Tris-acetate, 100 mM Mg(Ac)₂, and 1000 μg/ml recombinant albumin, pH 7.9 at 25°C], and 12 μl of water were added and incubated at 37°C for 60 min. Finally,

the solution was treated with 1.0 U/ μ l exonuclease I and 1.0 U/ μ l exonuclease III using a protocol similar to that described previously.

Cleavage of the dsDNA by *HinfI* and *BtsCI*

Typical protocol for digestion by *HinfI* (10 μ l total volume): 2.5 μ l of ligation products (0.2 μ M in 1 \times T4 DNA ligase buffer), 1 μ l of *HinfI* (0.5 U/ μ l or 10 U/ μ l), 1 μ l of rCutSmart buffer (10 \times), and 5.5 μ l of H₂O were mixed and incubated at 37°C for a specified duration (e.g. 30 min or 12 h). The final concentrations of ligation products, *HinfI*, and rCutSmart buffer were 0.05 μ M, 0.05 U/ μ l (or 4.0 U/ μ l), and 1 \times (50 mM KAc, 20 mM Tris-acetate, 10 mM Mg(Ac)₂, and 100 μ g/ml recombinant albumin, pH 7.9 at 25°C), respectively. Specific conditions for other experiments are provided in the figure captions.

Typical protocol for digestion by *BtsCI* (10 μ l total volume): 2.5 μ l of topoisomers (0.4 μ M in H₂O), 1 μ l of *BtsCI* (0.5 U/ μ l), 1 μ l of rCutSmart buffer (10 \times), and 5.5 μ l of H₂O were mixed. The reaction was incubated at 50°C for 30 min. The final concentrations of topoisomers and *BtsCI* were 0.1 μ M and 0.05 U/ μ l, respectively. Usually, a 0.5 pmol sample was analyzed on polyacrylamide gel with temperature control at 10–20°C.

Digestion of topoisomers by S1 nuclease

Typical protocol (10 μ l total volume): 2.5 μ l of topoisomers (4 μ M in H₂O), 1 μ l of S1 nuclease (0.1 U/ μ l), 2 μ l of S1 nuclease buffer (5 \times), and 4.5 μ l of H₂O were mixed. The reaction was incubated at 37°C for 30 min, and the enzyme was removed by extraction using phenol and chloroform. The final concentrations of topoisomers, S1 nuclease, and the buffer were 1.0 μ M, 0.01 U/ μ l, and 1 \times (200 mM sodium acetate, 1.5 M NaCl, and 10 mM ZnSO₄, pH 4.5), respectively.

Digestion of topoisomers by BAL31 nuclease

Typical protocol (10 μ l total volume): 2.5 μ l of topoisomers (4 μ M in H₂O), 1 μ l of BAL31 nuclease (0.001 U/ μ l), 5 μ l of BAL31 nuclease buffer (2 \times), and 1.5 μ l of H₂O were mixed. The reaction was incubated at 30°C for 30 min, and the enzyme was removed by extraction using phenol and chloroform. The final concentrations of topoisomers, BAL31 nuclease, and the buffer were 1.0 μ M, 0.0001 U/ μ l, and 1 \times [20 mM Tris-HCl, pH 8.0, 600 mM NaCl, 12 mM CaCl₂, 12 mM MgCl₂, 1 mM ethylenediaminetetraacetic acid (EDTA)], respectively.

Treatment of topoisomers with Topo-I

Typical protocol (10 μ l total volume): 2.5 μ l of topoisomers (0.4 μ M in H₂O), 1 μ l of Topo-I (0.1 U/ μ l), 1 μ l of rCutSmart buffer (10 \times), and 5 μ l of H₂O were mixed. The reaction was incubated at 37°C for 2 h. The final concentrations of topoisomers and Topo-I were 0.1 μ M and 0.01 U/ μ l, respectively. Specific conditions for other experiments are provided in the figure captions.

Measurement of T_m by HRM

The T_m values of topoisomers were determined by high-resolution melting (HRM) method [39]. Preparation of the sample (10 μ l total volume): 2.5 μ l of topoisomers (2.0 μ M in H₂O), 1 μ l of HEPES (100 mM, pH 7.0), 1 μ l of MgCl₂

(100 mM), 0.5 μ l of EvaGreen fluorescent dye (20 \times), and 5 μ l of H₂O were mixed. The final concentrations of topoisomers, HEPES, MgCl₂, and EvaGreen fluorescent dye were 0.5 μ M, 10 mM, 10 mM, and 1 \times , respectively. The mixture was annealed in a PikoReal Real-Time PCR instrument (Thermo Scientific, Finland) with a cooling rate of 0.1°C/s from 90°C to 10°C. The fluorescence data were collected over a temperature range of 10–95°C in 0.2°C increments. At least three parallel tests were made for one plate, and T_m values were calculated by the first derivatives of melting curves.

Gel shift assay for binding of topoisomers with antibody Z22

Typical protocol and conditions (10 μ l total volume): 2.5 μ l of topoisomers (0.40 μ M in H₂O), 1 μ l of HEPES (100 mM, pH 7.0), 1 μ l of MgCl₂ (100 mM), 2.5 μ l of Z-DNA-specific antibody (Z22) (0.20, 0.40, 0.80, or 1.60 μ M), and 3.0 μ l of H₂O were mixed. The reaction was incubated at 25°C for 2 h. The final concentrations of topoisomers, HEPES, MgCl₂, and Z22 were 0.5 μ M, 10 mM, 10 mM, and 0.25–2.0 μ M, respectively. The products of hybrids were analyzed by 12% native PAGE in 1 \times TBE running buffer (89 mM Tris, 89 mM boric acid, and 2.0 mM EDTA, pH 8.3) at 20°C.

Circular dichroism spectroscopy

The sample was prepared as follows (300 μ l total volume): 60 μ l of topoisomers (20 μ M in H₂O), 30 μ l of HEPES (100 mM, pH 7.0), 30 μ l of MgCl₂ (100 mM), and 180 μ l of H₂O were mixed and annealed (80°C for 3 min, 0.1°C/s cooling, 25°C for 30 min). The final concentrations of topoisomers, HEPES, and MgCl₂ were 4.0 μ M, 10 mM, and 10 mM, respectively. The spectra were recorded from 220 to 330 nm at the speed of 100 nm/min (JASCO Corporation, Japan). Quartz cuvette with path length of 1 mm was used. Each CD spectrum presented here was an average of at least five scans. Samples were equilibrated at each temperature for at least 3 min before the analysis. The baseline was calibrated with the corresponding buffer.

Difference spectra of Lk2 were obtained by subtracting 0.62 \times the spectrum of the corresponding Lk7 from the original spectrum of Lk2, considering that the length of the B-DNA portion in Lk is 62% of the total length (79 bp). The T_m of Z-DNA in Lk2 was obtained by calculating the first derivative of the curve reflecting the CD signal change at 295 nm.

Results

Molecular design and preparation of eight topoisomers of a 79-bp-long circular dsDNA

The isomers (Lk1–Lk6) of a 79-nt-long circular dsDNA are prepared using well-designed aid-DNAs as shown in Fig. 2 and Table 1. The circular ssDNAs of Cs and Ca are prepared from two fragments via a one-pot ligation approach (yield >95%) developed by our group (Supplementary Fig. S2) [37]. It is obvious that the topoisomer of Lk7 (linking number is 7) can be obtained by ligation after hybridization of Cs and La, as the pitch of the B-DNA duplex is \sim 10.4 bp. In fact, only one band of product (assigned as Lk7) was observed after ligation, demonstrating that the yield for Lk7 was almost 100% (lane 2 in Fig. 2D and E). When Cs and its circular comple-

Table 1. Lengths for ssDNA and dsDNA parts of Cs and La after hybridization with aid-DNAs

Strategy	Topoisomer	Cs (5'–3')				La (5'–3')			
		ssDNA for catenane ^a (nt)	dsDNA ^b (bp)	Unprotected ssDNA ^c (nt)	AidC (nt)	ssDNAs for catenane ^a (nt)	dsDNA ^b (bp)	Unprotected ssDNA ^c (nt)	AidL ^d (nt)
StrB	Lk1	10	32 + 32	5	64	10 + 10	20 + 20	19	20 + 20
	Lk2	20	27 + 27	5	54	10 + 10	20 + 20	19	20 + 20
	Lk3	30	22 + 22	5	44	15 + 15	20 + 20	9	20 + 20
	Lk4	45	14 + 15	5	29	22 + 23	18 + 16	0	39
StrA	Lk5	46	33	0	33	79	0	0	0
	Lk6	59	20	0	20	79	0	0	0

^aThe ssDNA for the catenane refers to the single-stranded region that is not protected by aid-DNAs. For La (StrB), there are two ssDNA regions ($x + y$), corresponding to the single-stranded portions near the 3' and 5' ends, respectively.

^bFor both Cs and La, there are two dsDNA parts ($x + y$) for StrB.

^cThe unprotected ssDNA is the ssDNA part after hybridization with aid-DNAs.

^dFor StrB (Lk1, Lk2, Lk3), two dsDNAs parts ($x + y$) are formed prior to ligation.

mentary strand (Ca) are mixed, Lk0 is obtained (with a yield close to 100%) consisting of a Z-DNA part and a B-DNA part, as reported previously [33].

The design principles for aid-DNAs used in the preparation of other topoisomers (Lk1–Lk6) are described as follows (Supplementary Fig. S3). By adjusting the length and sequence of aid-DNA to prevent unexpected hybridization, varying topoisomers (corresponding to the length of the hybridization part between Cs and La) can be obtained. Notably, longer aid-DNA results in a shorter hybridization part, and the obtained topoisomer has a smaller linking number (Fig. 1C and D). For an aid-DNA that is complementary to the circular ssDNA (Cs), it is designated as AidC, whereas one complementary to the linear ssDNA (La), designated as AidL. To prepare topoisomers with Lk1–Lk4, for example, one AidC and one (for Lk4) or two (for Lk1–Lk3) AidLs are used (StrB, Supplementary Fig. S3). For the preparation of Lk1, Lk2, Lk3, and Lk4, the expected lengths of hybridization parts between Cs and La are about 10, 21, 31, and 42 nt, respectively. The topoisomers of Lk5 or Lk6 are expected to be prepared by using only one short AidC (33 nt for Lk5, 20 nt for Lk6) on Cs (StrA). The expected hybridization lengths between Cs and La after constraining are ~52 and 63 nt, respectively (Supplementary Fig. S3).

In detail, for preparing topoisomers of Lk1–Lk6, the sequences of aid-DNAs were designed as shown in Fig. 2A–C and Table 1 (see also the sequence in Supplementary Table S1). Take Lk1 as an example (Fig. 2A): to remain a 10-nt-long ssDNA part in Cs and in La for hybridization to form the Lk1 topoisomer after ligation, AidC64 protects two 32-nt-long parts on Cs, and ^{C64}AidL^a and ^{C64}AidL^b protect two 20-nt-long parts on La. In ^{C64}AidL^a and ^{C64}AidL^b, the superscript of C64 indicates that these two aid-DNA strands work together with AidC64 to control the linking number. Before the hybridization of Cs and La, AidC64 forms two 32-bp-long duplexes with Cs, and ^{C64}AidL^a and ^{C64}AidL^b form two 20-bp-long duplexes with La to prevent undesired hybridization between Cs and La. After hybridization between Cs and AidC64, a 5-nt-long internal loop is designed to bend this 64-bp-long duplex so that the remaining 10-nt-long part is not so taut. Following the mixing of protected Cs and La in the presence of T4 DNA ligase, the hybridization between Cs and La as well as ligation (for end-sealing) occurs simultaneously, so that the topoisomer of Lk1 can form. For the preparation of the topoisomers of Lk5 and Lk6, only one AidC is

used (Table 1 and Fig. 2C), because they require protection of only 27-nt-long and 16-nt-long regions, respectively. As shown in Fig. 2C, longer protected regions (using AidC33 and AidC20) are designed to prevent complete displacement by unprotected La.

The ligation products were analyzed by dPAGE using strong denaturing conditions (25% formamide and 7.0 M urea) to dissociate the 79-nt-long duplex (Fig. 2D and E). A mixture of exonuclease I and exonuclease III was added to remove the linear ssDNAs (with free ends), and the undigested one should correspond to the circular ssDNA. In the experiments using AidC64, AidC54, AidC44, and AidC29 in StrB (together with corresponding aid-DNAs for La), several ligation products not digested by the two exonucleases were observed on 6% dPAGE (Fig. 2D), comparing lanes 3–6 (before digestion) with lanes 8–11 (after digestion). Based on the sequence design, at least four topoisomers of Lk1–Lk4 should be produced. From the difference in band intensity for these four cases, four ligation products (P1–P4) were distinguished, although we could not know their exact linking numbers only from these results.

For the case using AidC33 in StrA (with no aid-DNA for La), five new bands (P1–P5), including P3 and P4, were observed after ligation (Fig. 2D and E). Since P7 had the same mobility as Lk7 (see also lane 2 in Fig. 2D and E), it was assigned as the topoisomer of Lk7. As shown in Fig. 2F, for the case using AidC20 in StrA (with no aid-DNA for La), P6 was obtained as the main product (Supplementary Fig. S4), and it was assigned as Lk6 (see Figs 3 and 4). Therefore, all seven kinds of topoisomers (catenanes) may be produced.

Verification of obtained catenanes as topoisomers

To determine whether the prepared seven catenanes (circular dsDNAs) are topoisomers with different linking numbers, we used the restriction enzyme *Hinf*I to check whether their digested products were the same (Fig. 3A). As shown in Fig. 3B, these catenanes had similar mobility on the native PAGE, suggesting that they were topoisomers but not polymers of catenanes (see also Supplementary Fig. S5A). After 30 min of digestion by 0.05 U/μl *Hinf*I, the catenanes supposed to have higher linking numbers were digested much more rapidly than those with smaller linking numbers (comparing lanes 10–17 with lanes 4–9, Fig. 3B), which is reasonable probably because digestion is more challenging for catenanes with a higher ra-

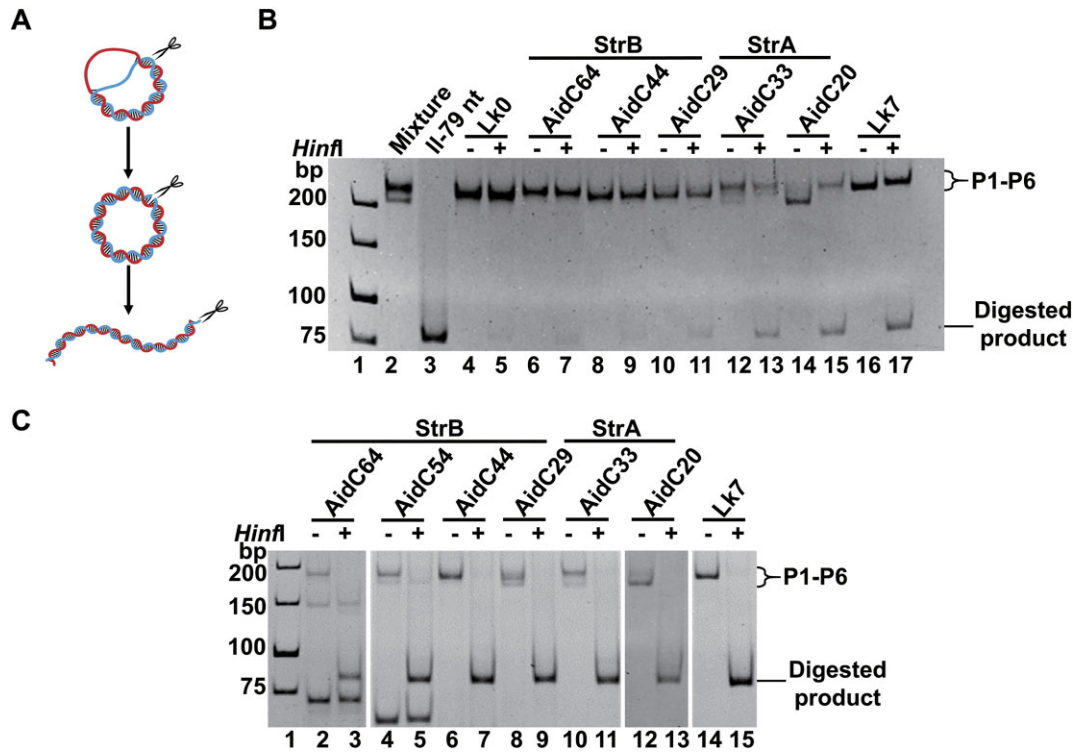


Figure 3. Verification of obtained circular dsDNA as topoisomers. **(A)** Diagram illustrating the digestion of circular dsDNAs by restriction enzyme *HinfI*, with a nicked structure as the intermediate. **(B)** Analysis of cleaved products by *HinfI* (8% PAGE). Lane 1: DNA ladder; lane 2: a mixture of all the obtained circular dsDNA after digestion by exonucleases; lane 3: linear 79-bp dsDNA; lanes 4, 6, 8, 10, 12, 14, and 16: circular dsDNA before digestion by *HinfI*; lanes 5, 7, 9, 11, 13, 15, and 17: after digestion by *HinfI*. Conditions: 0.05 μ M circular dsDNA, 0.05 U/ μ l *HinfI*, 37°C for 30 min. **(C)** Analysis of products cleaved by *HinfI* under more stringent conditions (4.0 U/ μ l *HinfI* at 37°C for 12 h). Other conditions and lane arrangements are the same as shown in panel (B).

tio of Z-DNA parts [33]. Similar results were also observed under varying conditions (Supplementary Fig. S5B).

Interestingly, for P6 (in the case of AidC20), two new bands appeared after digestion (lane 15 in Fig. 3B). The band with higher mobility runs with the same speed as other lanes (comparing lane 15 to lanes 13 and 17 in Fig. 3B), and the other band shows much lower mobility, even lower than that before digestion (comparing lane 15 to lane 14). When dPAGE containing 8.0 M urea (without formamide) was used, two bands were also observed (Supplementary Fig. S5B). The band with lower mobility could be assigned as circular dsDNA with a nick, similar to a nicked plasmid. Given that the length is only 79 bp and the DNA is highly rigid, the nucleotides flanking the nick may dissociate due to the strong stress, making further digestion by *HinfI* more difficult. After 12 h of digestion by 4.0 U/ μ l *HinfI*, as expected, almost all catenanes were digested completely, and the products had the same mobility (Fig. 3C). The digestion products exhibited higher mobility on the gel, because the circular dsDNA changed to linear dsDNA by dsDNA cleavage. These results show that all these catenanes are topoisomers with varying linking numbers.

Separation of topoisomers and determination of their linking numbers

To determine the topology (linking number) of each topoisomer, these isomers must be separated and, if necessary, purified. Fortunately, mobility for topoisomers of short ssDNA

catenanes varies greatly with their linking numbers on dPAGE of varying concentrations, which can be used as the basis for determining the linking number [40, 41]. At low concentration (4%) of dPAGE, the topoisomers with higher linking numbers (more compact structure) migrate more rapidly, whereas at higher concentration (e.g. >10%) of dPAGE, the topoisomers with smaller linking numbers migrate more slowly in some cases [40, 41]. Fig. 4 shows our results for further analysis and characterization of topoisomers (see also Supplementary Fig. S6).

As shown in Fig. 4A, all seven topoisomers (Lk1–Lk7) were separated by using 4% dPAGE, although Lk1 showed only slightly lower mobility than Lk2 (lane 4). According to previously reported findings [40, 41], and the information shown in Fig. 2D–F, the linking numbers of all topoisomers were temporarily determined as shown labeled at the right side of Fig. 4A. Similar results (larger Lk gives higher mobility) were also obtained using 6% dPAGE (Fig. 2D). However, for 10% dPAGE, topoisomers of Lk1, Lk2, Lk3, and Lk4 show similar mobility (difficult to separate) (Fig. 4B). When 20% dPAGE was used, all topoisomers could also be separated, but the difference between each two isomers is very small even after running for 40 h (Supplementary Fig. S6C). These results are consistent with the above linking number determination. On the other hand, these results demonstrate again that it is difficult to separate all of them clearly using a single PAGE. In some cases, the interference of Cs and Ca must be considered (Supplementary Fig. S6D). The relative mobilities of Lk1–Lk7 on dPAGE of varying concentrations are summa-

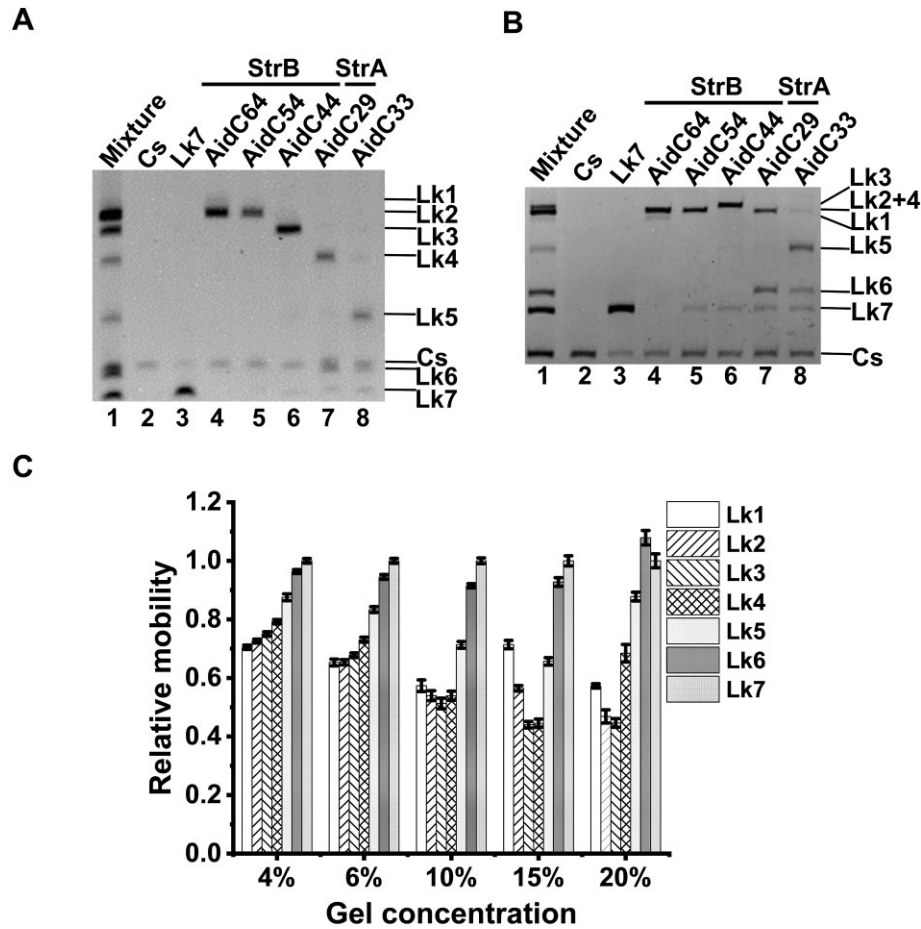


Figure 4. Separation of Lk1–Lk7 topoisomers by 4% dPAGE containing 8.0 M urea (**A**) or 10% dPAGE containing 25% formamide and 7.0 M urea (**B**). The relative mobility of Lk1–Lk7 on dPAGE of varying concentrations is shown in panel (**C**). Other conditions are the same as shown in Fig. 2. The relative mobility was calculated as follows: relative mobility = (mobility of topoisomer)/(mobility of Lk7). At least three parallel tests were conducted. The error bar represents the standard deviation.

rized in Fig. 4C. It is noteworthy that Lk1 and Lk2 showed higher mobility than Lk3 on dPAGE of higher concentrations (10%–20%).

The selectivity for preparing each topoisomer is shown in Table 2. For Lk2, Lk3, Lk4, and Lk7, the selectivity can be higher than 75%, demonstrating that the topological control was very successful. The highest selectivity for preparing Lk5 was 52.0% with StrA using AidC33 (Table 2). For preparing Lk1, the most difficult one, the selectivity was only about 10% when using AidC64 (StrB). By using AidC104, a 104-nt-long aid-DNA containing five phosphorothioated modifications (Fig. 5A and C), the selectivity was improved to 31.6% (Fig. 5E). It is noteworthy that AidC104 was circularized by T4 DNA ligase to utilize the topological constraint for preventing undesired strand displacement. After circularization of La to form the Lk1 catenane, circularized AidC104 was linearized by using I₂ at the phosphorothioated sites, as we reported previously [38], followed by removal with exonucleases.

To improve the selectivity for preparing Lk5, we further designed a long aid-DNA of AidC69 (Fig. 5B and D), which is circularized after hybridization using Cs as the template. AidC69 first hybridizes to C⁶⁹AidA, leaving a 15-nt ssDNA region at each end. These two 15-nt regions can then hybridize with Cs (as the scaffold) and be sealed by T4 DNA ligase. Ac-

Table 2. Selectivity of topoisomers prepared by StrA and StrB

Method		Selectivity (%) ^a							
		Lk0	Lk1	Lk2	Lk3	Lk4	Lk5	Lk6	Lk7
StrB	AidC64	0	10.9	88.2	0	0	0	0	0.88
	AidC54	0	0	92.4	0	0	0	0	7.6
	AidC44	0	0	2.9	92.6	0	1.11	0	3.4
	AidC29	0	0	0	3.04	75.8	0.89	14.6	5.8
StrA	AidC33	0	0	0	2.42	12.3	52.0	17.1	16.1
	AidC20	0	0	0	0	1.7	3.7	91.3	3.4
StrC	AidC104	0	31.6	35.0	28.5	0	0	0	4.8
StrD	AidC69	0	0	0	3.7	15.7	80.7	0	0
No aid-DNA		0	0	0	0	0	0	0	100
Mix Cs and Ca		100	0	0	0	0	0	0	0

^aSelectivity = (yield of each topoisomer)/(yield of all topoisomer). Six parallel experiments were performed for each sample, and the average value was used. The standard deviations ranged from 0.2% to 6.0%.

cordingly, circularized AidC69 (forming a catenane with Cs) is resistant to displacement by La due to the topological constraint. Then, the 59-nt ssDNA region on La (after being protected by C69AidL) hybridizes with Cs to form a 49-bp duplex with a nick, which is further sealed by T4 DNA ligase. Finally, the circularized AidC69 is cleaved by *Eco*RI, followed by removing with exonucleases (Fig. 5B and D). As shown in Fig. 5F, the selectivity was improved to 80.7% (Table 2).

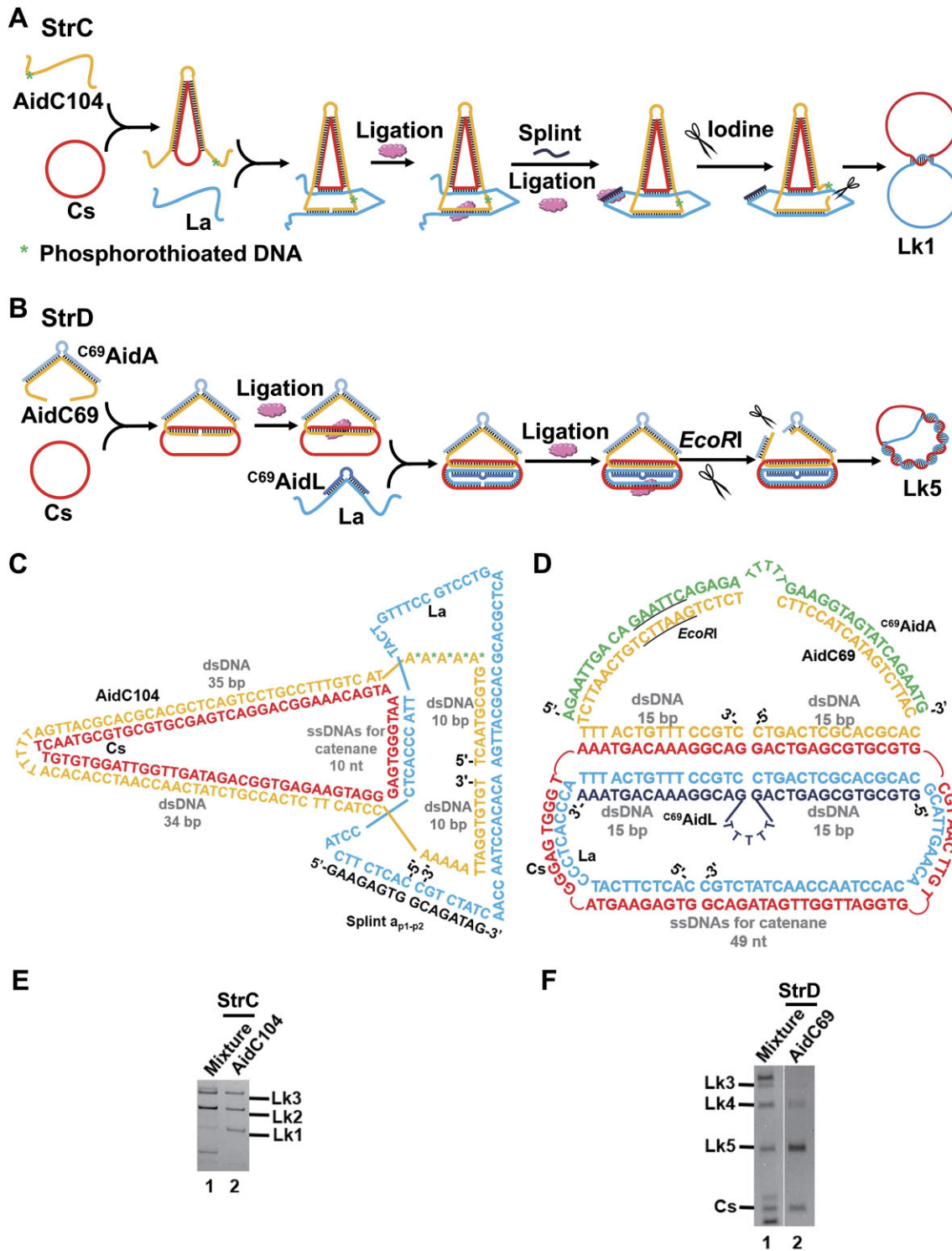


Figure 5. Preparation of Lk1 (A, C, E) and Lk5 (B, D, F) with higher selectivity. **(A)** Diagram of strategy C (StrC) for preparing Lk1. AidC104 (containing five continuous phosphorothioated modification sites) is circularized after hybridization, followed by cleavage using I_2 . **(B)** Diagram of strategy D (StrD) for preparing Lk5. The aid-DNA of AidC69 (containing the recognition site of restriction enzyme *EcoRI*) is circularized after hybridization, followed by cleavage with *EcoRI*. C⁶⁹AidA was used to prevent AidC69 from winding onto Cs. **(C)** Sequence design for preparing Lk1. **(D)** Sequence design for preparing Lk5 (49 nt on Cs are left for hybridization of La). **(E)** dPAGE (15%) analysis of prepared Lk1. **(F)** dPAGE (6%) analysis of prepared Lk5.

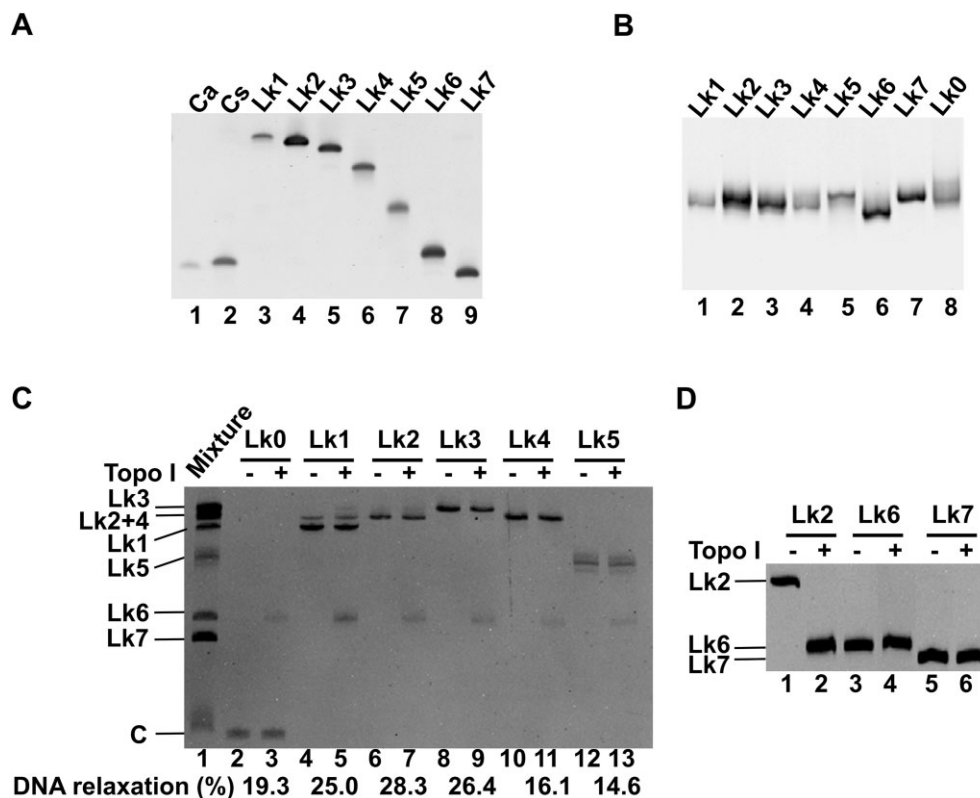


Figure 6. Electrophoresis of prepared topoisomers (A, B) and their treatment with Topo-I (C, D). (A) dPAGE (6%) for Lk0–Lk7. (B) Non-denaturing PAGE (8%, 20°C) for Lk0–Lk7. (C) Results for Lk1–Lk5 (0.10 μM) after treatment with Topo-I (0.01 U/μl Topo-I, 37°C, 2 h). (D) Results for Lk2, Lk6, and Lk7 (0.20 μM) (2.0 U/μl Topo-I, 37°C, 12 h).

Purification of topoisomers and their digestion by Topo-I

After purification by gel cutting and recovery of separated topoisomers, they were analyzed using 6% dPAGE (Fig. 6A), demonstrating that all these seven topoisomers (Lk1–Lk7) were obtained with high purity (single band). On an 8% non-denaturing PAGE, the difference in mobility of Lk0–Lk7 (eight topoisomers) was much smaller, indicating that their shapes and sizes are similar, demonstrating again that they are topoisomers (Fig. 6B). Interestingly, Lk6 showed higher mobility (lane 6, Fig. 6B), probably because this circular dsDNA has a different shape or partially dissociates due to the strong topological constraint (Fig. 7A).

Treatment of these topoisomers with Topo-I was also carried out (Fig. 6C and D). Topo-I can cut one of the two strands of dsDNA, relax the stress, and reseal the nick. As expected, for Lk0–Lk5 with strong stress to unwind part of this dsDNA (similar to the plasmid with high superhelical density), a new product with the same mobility as Lk6 was obtained after Topo-I's catalysis (Fig. 6C). For both Lk6 and Lk7, no change was observed even under much more stringent conditions (Fig. 6D). Obviously, topoisomers can be transferred to Lk6 (with a similar topological stress as normal genome dsDNA *in vivo*) by Topo-I. Under more stringent conditions, a high yield of Lk6 was obtained from Lk0–Lk5, although some differences can be observed (Supplementary Fig. S7).

Z-DNA can form for Lk1–Lk6

In our previous studies, we reported that Lk0 topoisomer forms a chimera consisting of a Z-DNA (left-handed DNA)

part and a B-DNA (right-handed DNA) part even under low ionic strength (e.g. 1.0 M MgCl₂) [15, 33]. In fact, we introduced to Cs and La a 12-bp-long APP sequence (5'-TGC GTGCGT GCG-3'/5'-CGCACGCACGCA-3') that readily adopts Z-conformation (Fig. 1A and Supplementary Table S1). Accordingly, we are interested in determining whether Lk1–Lk6 can form partially Z-DNA structures (Fig. 7A). The topoisomers of Lk4–Lk7 can reflect the *in vivo* situation of genome dsDNA to some extent with varying superhelical density (4–6). The formation of Z-DNA was checked by gel shift assay using Z22, an antibody specifically binding to Z-DNA (Fig. 7B). For Lk1–Lk5, the band intensity of the topoisomers gradually decreased as the ratio of antibody to topoisomers increased, which is consistent with our previous findings (Fig. 7B and Supplementary Fig. S8). Interestingly, the binding of Z22 was also observed for Lk6 (0.1 μM), although it occurred only at higher concentrations of Z22 (0.2 or 0.4 μM, 1:2 or 1:4, lanes 21–25). This result is particularly noteworthy because the Z-DNA part, if formed, is only 7 or 8 bp long (Table 3). Table 3 summarizes the lengths of B-DNA and Z-DNA in Lk0–Lk6 in theory. After incubation at high temperature (>85°C), the band of topoisomers (not binding to Z22) reappeared, likely due to dissociation and denaturation of Z22 (lanes 3 and 4 in Supplementary Fig. S8). As expected, no binding was observed for Lk7 (lane 6 in Supplementary Fig. S8).

The formation of Z-DNA in Lk2 and Lk6 (using Lk7 as the control) was also confirmed by measuring circular dichroism (CD) at 20°C (Fig. 7C). After subtracting the CD signal of B-form DNA in Lk2, the difference spectrum (red line) displayed a pattern similar to that of Z-DNA, which was also observed previously (the positive Cotton at 264 nm and the

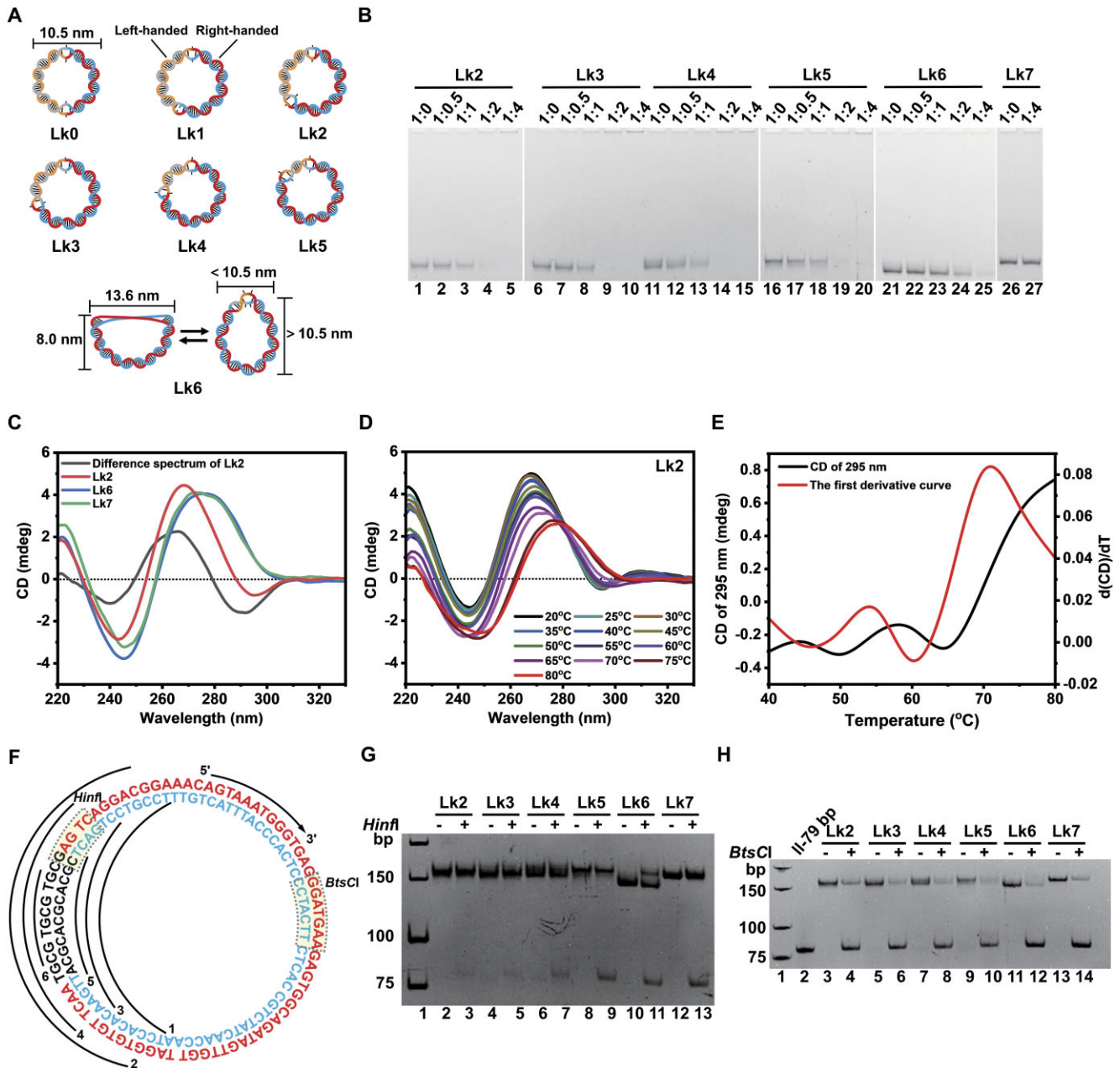


Figure 7. Assessment of Z-DNA formation and its position in topoisomers. **(A)** Structures of topoisomers containing Z-DNA parts of varying lengths. **(B)** Gel shift assay for the binding of Z22 to topoisomers. Conditions: 0.1 μ M topoisomers; molar ratio (topoisomer to Z22): 1:0.5, 1:1, 1:2, or 1:4; incubated at 25°C for 2 h; 12% PAGE (20°C). **(C)** CD spectra of Lk2, Lk6, and Lk7 at 20°C. The difference spectrum (CD of Z-DNA segment in Lk2 (CD_{Lk2} - 0.62 \times CD_{Lk7}) is shown (red line), and a typical CD spectrum of Z-DNA was obtained. **(D)** CD of Lk2 at varying temperatures (20–80°C). **(E)** Change of CD values for Lk2 at 295 nm with temperature, and the first derivative curve with a peak (T_m) at 71.0°C. **(F)** Proposed positions of Z-DNA. The black arcs represent the regions of Z-DNA sequences in each topoisomer (the number indicates the linking number). The recognition sites of the restriction enzymes *Hinfi* and *BtsCI* are shown in dashed boxes. The black letters represent the APP sequences. **(G, H)** Digestion results (12% PAGE) for *Hinfi* and *BtsCI*, respectively. Conditions: 0.1 μ M topoisomer, 0.05 U/ μ l *Hinfi* or *BtsCI*, incubated at 37°C (*Hinfi*) or 50°C (*BtsCI*) for 30 min.

negative Cotton at 295 nm) [15, 33]. From the CD spectrum change with temperature (Fig. 7D) and the CD value at 295 nm with temperature (Fig. 7E), the melting temperature (T_m) of Lk2 was 71.0°C. These results demonstrate that Z-DNA in Lk2 remains stable at least below 60°C, because the CD signal belonging to Z-DNA was clearly observed at this temperature (Fig. 7D). However, for Lk6, no obvious difference was observed compared with Lk7, indicating that the potentially formed 7- or 8-bp-long Z-DNA may not be so stable (Table 3), and exists in equilibrium between partial dissocia-

tion and Z-DNA formation (Fig. 7A). It is also consistent with the results shown in Fig. 7B; i.e. Z22 can bind to Lk6 and stabilize the Z-DNA duplex at higher concentrations of Z22. The structures of Lk0–Lk5 and Lk7 are presumed to be ring- or fusiform-shaped, with a diameter of \sim 10.5 nm.

Interestingly, no obvious CD change (neither wavelength shift nor CD values) with temperature within the range of 20°C–80°C was observed for Lk6 (Supplementary Fig. S9A). It indicates that the thermal stability of Lk6 is above 80°C at least partially (e.g. a part of the 20-bp segment dissociates, and

Table 3. Calculated Z-DNA length of topoisomers prepared by StrA and StrB

Topoisomer ^a	Lk0	Lk1	Lk2	Lk3	Lk4	Lk5	Lk6	Lk7
Turn number of Z-DNA	3.5	3.0	2.6	2.0	1.6	1.2	0.7	0
Length of Z-DNA (bp)	42	36	30	24	20	14	7 or 8	0
Length of B-DNA (bp)	35	41	47	53	57	63	69	74
Superhelical density ^b	–	–0.87	–0.73	–0.60	–0.47	–0.33	–0.20	–0.067

^aTwo B–Z junctions (1 bp each) are present for Lk0–Lk6.

^bCalculated using $(Lk - Lk_0)/Lk_0$ ($Lk_0 = 7.5$). The values of superhelical density do not reflect the real density (number) of the supercoils.

the remaining 59-bp duplex forms). It is noteworthy that Lk6 (an ssDNA catenane) should have a T_m even higher than a linear 59-bp dsDNA, because the two strands of Lk6 cannot separate freely even after complete melting. More interestingly, an obvious CD change was observed for Lk7 within the range of 220–260 nm, when the temperature increased from 65°C to 75°C (Supplementary Fig. S9B). This suggests that part of Lk7 (e.g. 20 bp) may dissociate (with a similar structure as Lk6, but the dissociate parts also wind in a right-handed way and contribute to the linking number) at temperatures above 65°C, due to the strong bending stress in the mini-dsDNA of only 79 bp (Supplementary Fig. S9C).

It is well known that, compared with non-APP sequences, APP sequences prefer to form Z-DNA, as the APP sequence promotes the formation of alternating *anti* and *syn* conformations corresponding to the glycosidic bonds. Accordingly, we hypothesize that Z-DNA is formed preferably around the APP sequence (Fig. 7F). Two restriction endonucleases (*Hinf*I and *Bts*CI) were used to preliminarily determine the position of the Z-DNA part (difficult to digest compared with B-DNA). As expected, the digestion was more difficult for Lk0–Lk4 compared with Lk5–Lk7 by *Hinf*I, whose recognition site is close to the APP sequence (Fig. 7G). On the other hand, no obvious difference was observed for digestion by *Bts*CI, whose recognition site is at the position far from the APP site (Fig. 7H). We also tried the digestion by S1 nuclease and BAL 31, two ssDNA-specific endonucleases. Compared with Lk7, all other topoisomers were digested more easily, demonstrating that the B–Z junction can be specifically digested by ssDNA-specific endonucleases (Supplementary Fig. S10). No obvious difference was observed for topoisomers of Lk1 to Lk6. The result that no random digestion was observed for Lk6 indicates that the Z-DNA may also form, at least to some extent, at 37°C (the temperature for S1 digestion). Collectively, the Z-DNA part (14–36 bp) can form under physiological ionic conditions (around the APP sequence) for topoisomers of Lk1–Lk5. For Lk6, Z-DNA can form but not so stable.

Discussion

In this study, as a model of a short dsDNA circle with different topological constraints, we prepared, for the first time, all the topoisomers (Lk0–Lk7) of a 79-bp-long circular dsDNA by using aid-DNA to prevent undesired hybridization. All these topoisomers were separated by PAGE and purified (Fig. 4). Compared with longer circular dsDNA, the 79-bp one is very difficult to form negative supercoils (neither the toroid style nor the plectoneme style) due to the rigidity of dsDNA (with the persistence length of 50 nm or 150 bp), so that allow-

ing us to simplify the structural analysis (e.g. mainly considering the partial formation of Z-DNA or dissociation). For a longer circular dsDNA like a plasmid, the topology is more easily transmitted or converted to other forms. The topoisomers we constructed can be used to study the effect of superhelical density on the structure of dsDNA, including unwinding or Z-DNA formation. Accordingly, we overcame significant challenges and completed this challenge. Obviously, our approach offers advantages over previously reported methods [32, 35, 36].

Because two strands (79 nt) are fully complementary, strict control over the linking number or hybridization length is extremely difficult due to the strand displacement by aid-DNA. The timing of ligation is very important but difficult to control. If the ligation is too slow, strand displacement occurs; if the ligation is too fast, insufficient hybridization between Cs and La occurs. In addition, even when the hybridization is strictly controlled, the Lk can also change (± 1) depending on the direction in which one strand (La) stretches below or above another strand (Cs) (Supplementary Fig. S3G). As a result, even in the presence of aid-DNAs, selectivity >90% was only achieved for Lk2, Lk3, and Lk6 besides Lk0 and Lk7 (Table 2). The relative simplicity for preparing Lk2 and Lk3 can be explained by the large length difference between the duplex for protection and the duplex for forming the catenane (Figs 2 and 3). The long protecting duplex formed with aid-DNA is difficult to displace due to its high stability. Unexpectedly, high selectivity (91.3%) of Lk6 was obtained, although the duplex for protection was only 20 bp, probably because the strand displacement was slow due to the topological disadvantage. However, for other topoisomers of Lk1, Lk4, and Lk5, only mixtures (containing at least two undesired topoisomers) were obtained even under the protection of well-designed aid-DNAs. Although StrB is more suitable for the preparation of smaller Lk topoisomers, two aid-DNAs are required to protect each strand. We tried to use only one longer AidC as StrA, a variety of redundant topological isomers appeared (data not shown). Fortunately, the selectivity for Lk1 and Lk5 was improved greatly by using a newly designed strategy using the topological constraint by circularizing the aid-DNA during the preparing process (Fig. 5).

The characterization of the linking numbers of the produced topoisomers is based on the following facts. At first, a higher linking number corresponds to higher mobility on 4% dPAGE (Fig. 6A), when the denaturing conditions are strong enough (in the presence of 30% formamide), which has also been confirmed by several reports [40, 41]. Second, Lk7 can be determined, because the largest linking number for a 79-nt-long is 7 when spontaneously ligated. Third, Lk6 could also be determined, because all topoisomers with a smaller linking number were converted to this structure by Topo-I. When calculating using the formula of $(Lk - Lk_0)/Lk_0$, the superhelical density of Lk6 is $\sim -20\%$. Fourth, it is well known that Lk1 is difficult to obtain, because a duplex of 10 bp is not stable enough. Only 31.6% selectivity was achieved after using the strategy shown in Fig. 5A. Accordingly, it can be determined as Lk1. The remaining four bands should be corresponding to Lk2–Lk5 (Fig. 6A).

It is interesting that the six topoisomers of Lk0–Lk5 can be converted by Topo-I to Lk6, demonstrating that they are the substrates of this enzyme. In other words, these results demonstrate that these topoisomers do not form unusual structures that Topo-I cannot bind. This is further supported by the fact

that they can be digested by a restriction enzyme. It is noteworthy that these topoisomers are typically nicked by the restriction enzyme initially because of the strong binding stress, before both strands are cut, as has been previously reported [42]. This is clearly illustrated by the results shown in Fig. 7G (lane 11). Considering that very high superhelical density (referring to the absolute value) may occur during DNA replication and transcription, these topoisomers can be used as a model to study the *in vivo* characteristics of topoisomerases.

As we reported previously for Lk0 [15, 33], topoisomers of Lk1–Lk6 can also partially form Z-DNA due to topological constraints, although a higher concentration of Z22 was required to observe the gel shift for Lk6 (Fig. 7B–E). Only 7–8-bp Z-DNA can form, and this may be the reason that obvious signals of Z-DNA were observed for Lk6. Because the T_m values were above 60°C in most cases, we believe that Z-DNA forms first before the binding of Z22. Even for Lk6, Z22 can stabilize the Z-DNA after binding, but does not induce Z-DNA formation. It is well known that Z22 cannot bind to B-DNA duplex under normal concentrations. It can be inferred that the local high superhelical density caused by transcription (or replication) may be relieved by forming Z-DNA (not necessary to be APP sequence). The formation of a Z-DNA duplex can improve the stability of genome DNA compared with the ssDNA state. These Z-DNA regions can later be converted to B-DNA by Topo-I. On the other hand, if the Z-to-B transition does not occur in a timely manner, the transcribed RNA may invade, leading to the formation of an R-loop.

The T_m values were also measured for all topoisomers of Lk0–Lk7 by HRM within the range of 20–80°C (Supplementary Fig. S11). For Lk0, a clear sigmoid shape of the melting curve was observed with a T_m of ~69°C (Supplementary Fig. S11A). In contrast, the sigmoid shapes were less pronounced for the other topoisomers, and what we could know is that their T_m values were all above 60°C, but precise values could not be obtained. A possible explanation is that, even after partially melting, a dynamic equilibrium of duplex formation and dissociation occurs at varying positions (similar to a bubble moving around within the duplex). We believe that the duplex only dissociates partially even at 80°C, because the two strands in single-strand state can still wind around each other in right-handed, left-handed, or parallel manner (Supplementary Fig. S12). It is noteworthy that the dye (EvaGreen) we used cannot bind strongly at a temperature above 80°C, even if the duplex forms stably.

At present, there is almost no effective method to study the effect of DNA topology on molecular biological processes, such as R-loop formation [44, 45]. On the other hand, it is well known that dsDNA must open and form bubbles to some extent for replication, transcription, gene regulation, and even for chromatin remodeling. The structures we have constructed are a type of mimicry of these bubbles with varying lengths or topological stress strengths. For example, if the bubble is too big, the possibility of R-loop formation may increase significantly. This may explain why Lk2 cannot transcribe efficiently, although the short R-loop (if formed) is not stable enough to inhibit transcription (Supplementary Fig. S13). In contrast, both Lk6 and Lk7 can transcribe efficiently, indicating that transcription can initiate without the promoter [43]. One possibility is that the promoter merely serves to position the transcription start site. Once a bubble is generated, the transcription can occur, which is partly supported by our model.

In summary, we used a short circular dsDNA of 79 bp as a model to prepare eight topoisomers with varying linking numbers (0–7) by using well-designed aid-DNAs to prevent undesired hybridization prior to ligation. Except for Lk1, all other topoisomers were obtained with a selectivity above 75%. For Lk2, Lk3, and Lk6, the selectivity exceeded 90%. All topoisomers were separated and purified by PAGE, and they can be used as excellent materials for studying DNA topology. Topoisomers of Lk0–Lk1 can form a partially Z-DNA conformation, which are stable at ionic strengths close to those in the cellular environment. Clarification of the biological functions of topological constraints, as well as Z-DNA, becomes possible using our strategy. These topoisomers also hold promise as materials for the diagnosis or therapy of Z-DNA-related diseases.

Acknowledgements

Author contributions: Mengqin Liu (Conceptualization, Data curation, Formal analysis, Methodology, Writing—original draft), Ziyi Wang (Data curation, Methodology, Writing—review), Ran An (Formal analysis, Funding acquisition, Writing—review & editing), Angda Li (Writing—review & editing), and Xingguo Liang (Conceptualization, Formal analysis, Funding acquisition, Methodology, Writing—review & editing).

Supplementary data

Supplementary data is available at NAR online.

Conflict of interest

None declared.

Funding

This work was supported by National Natural Science Foundation of China Youth Program (32102064 to R.A.), Qingdao Natural Science Foundation (24-4-4-zrjj-147-jch to L.X.), and Open Foundation of State Key Laboratory of Marine Food Processing & Safety Control (SKL202308 to R.A.). Funding to pay the Open Access publication charges for this article was provided by Qingdao Natural Science Foundation.

Data availability

The data underlying this article will be shared on reasonable request to the corresponding author.

References

- Mulholland N, Xu Y, Sugiyama H *et al.* SWI/SNF-mediated chromatin remodeling induces Z-DNA formation on a nucleosome. *Cell Biosci* 2012;2:1. <https://doi.org/10.1186/2045-3701-2-3>
- Zhang F, Huang Q, Yan J *et al.* Histone acetylation induced transformation of B-DNA to Z-DNA in cells probed through FT-IR spectroscopy. *Anal Chem* 2016;88:4179–82. <https://doi.org/10.1021/acs.analchem.6b00400>
- Achar YJ, Adhil M, Choudhary R *et al.* Negative supercoil at gene boundaries modulates gene topology. *Nature* 2020;577:701–5. <https://doi.org/10.1038/s41586-020-1934-4>

4. Shin SI, Ham S, Park J *et al.* Z-DNA-forming sites identified by ChIP-Seq are associated with actively transcribed regions in the human genome. *DNA Res* 2016;23:477–86. <https://doi.org/10.1093/dnares/dsw031>
5. Wang G, Vasquez KM. Z-DNA, an active element in the genome. *Front Biosci* 2007;12:4424–38. <https://doi.org/10.2741/2399>
6. Huang S, Fu Q, Cheng F *et al.* d(GC)₁₀ sequence within promoter region enhances the promoter activity in *Saccharomyces cerevisiae*. *ABBS* 2018;50:1288–90. <https://doi.org/10.1093/abbs/gmy134>
7. Inagaki H, Ohye T, Kogo H *et al.* Two sequential cleavage reactions on cruciform DNA structures cause palindrome-mediated chromosomal translocations. *Nat Commun* 2013;4:1592. <https://doi.org/10.1038/ncomms2595>
8. Lu G, Ferl RJ. Site-specific oligodeoxynucleotide binding to maize Adh1 gene promoter represses Adh1-GUS gene expression *in vivo*. *Plant Mol Biol* 1992;19:715–23. <https://doi.org/10.1007/BF00027068>
9. Vetcher AA, Wells RD. Sticky DNA formation *in vivo* alters the plasmid dimer/monomer ratio. *J Biol Chem* 2004;279:6434–43. <https://doi.org/10.1074/jbc.M309595200>
10. Wang R, Li H, Wu J *et al.* Gut stem cell necroptosis by genome instability triggers bowel inflammation. *Nature* 2020;580:386–90. <https://doi.org/10.1038/s41586-020-2127-x>
11. Zhang T, Yin C, Boyd DF *et al.* Influenza virus Z-RNAs induce ZBP1-mediated necroptosis. *Cell* 2020;180:1115–29. <https://doi.org/10.1016/j.cell.2020.02.050>
12. Jiao H, Wachsmuth L, Wolf S *et al.* ADAR1 averts fatal type I interferon induction by ZBP1. *Nature* 2022;607:776–83. <https://doi.org/10.1038/s41586-022-04878-9>
13. Jiao H, Wachsmuth L, Kumari S *et al.* Z-nucleic-acid sensing triggers ZBP1-dependent necroptosis and inflammation. *Nature* 2020;580:391–5. <https://doi.org/10.1038/s41586-020-2129-8>
14. Lei Y, VanPortfliet JJ, Chen Y *et al.* Cooperative sensing of mitochondrial DNA by ZBP1 and cGAS promotes cardiotoxicity. *Cell* 2023;186:3013–32. <https://doi.org/10.1016/j.cell.2023.05.039>
15. Li L, Zhang Y, Ma W *et al.* Nonalternating purine pyrimidine sequences can form stable left-handed DNA duplex by strong topological constraint. *Nucleic Acids Res* 2022;50:684–96. <https://doi.org/10.1093/nar/gkab1283>
16. Shure M, Vinograd J. The number of superhelical turns in native virion SV40 DNA and minicircle DNA determined by the band counting method. *Cell* 1976;8:215–26. [https://doi.org/10.1016/0092-8674\(76\)90005-2](https://doi.org/10.1016/0092-8674(76)90005-2)
17. Singleton CK, Wells RD. The facile generation of covalently closed, circular DNAs with defined negative superhelical densities. *Anal Biochem* 1982;122:253–7. [https://doi.org/10.1016/0003-2697\(82\)90277-9](https://doi.org/10.1016/0003-2697(82)90277-9)
18. Wang Z, Harshey RM. Crucial role for DNA supercoiling in Mu-transposition: a kinetic study. *Proc Natl Acad Sci USA* 1994;91:699–703. <https://doi.org/10.1073/pnas.91.2.699>
19. Haq S, Natori S, Sekimizu K. Heat-induced DNA relaxation *in vitro* by mouse DNA topoisomerase I in the presence of ethidium bromide. *J Biochem* 1993;113:620–4. <https://doi.org/10.1093/oxfordjournals.jbchem.a124092>
20. Anderson BG, Stivers JT. Variola type IB DNA topoisomerase: DNA binding and supercoil unwinding using engineered DNA minicircles. *Biochemistry* 2014;53:4302–15. <https://doi.org/10.1021/bi500571q>
21. Pyne ALB, Noy A, Main KHS *et al.* Base-pair resolution analysis of the effect of supercoiling on DNA flexibility and major groove recognition by triplex-forming oligonucleotides. *Nat Commun* 2021;12:1053. <https://doi.org/10.1038/s41467-021-21243-y>
22. Fogg JM, Kolmakova N, Rees I *et al.* Exploring writhe in supercoiled minicircle DNA. *J Phys Condens Matter* 2006;18:S145–59. <https://doi.org/10.1088/0953-9884/18/14/S01>
23. Irobalieva RN, Fogg JM, Catanese DJ Jr *et al.* Structural diversity of supercoiled DNA. *Nat Commun* 2015;6:8440. <https://doi.org/10.1038/ncomms9440>
24. Saintome C, Delagoutte E. Probing hyper-negatively supercoiled mini-circles with nucleases and DNA binding proteins. *PLoS One* 2018;13:e0202138. <https://doi.org/10.1371/journal.pone.0202138>
25. Glikin GC, Jovin TM, Arndt-Jovin DJ. Interactions of drosophila DNA topoisomerase-II with left-handed Z-DNA in supercoiled minicircles. *Nucl Acids Res* 1991;19:7139–44. <https://doi.org/10.1093/nar/19.25.7139>
26. Waszkiewicz R, Ranasinghe M, Fogg JM *et al.* DNA supercoiling-induced shapes alter minicircle hydrodynamic properties. *Nucleic Acids Res* 2023;51:4027–42. <https://doi.org/10.1093/nar/gkad183>
27. Hobson MJ, Bryant Z, Berger JM. Modulated control of DNA supercoiling balance by the DNA-wrapping domain of bacterial gyrase. *Nucleic Acids Res* 2020;48:2035–49. <https://doi.org/10.1093/nar/gkz1230>
28. Li D, Wang Q, Zhou B *et al.* Small DNA circles as bacterial topoisomerase I inhibitors. *RSC Adv* 2019;9:18415–9. <https://doi.org/10.1039/C9RA02398D>
29. Ahmed SM, Drge P. Chromatin architectural factors as safeguards against excessive supercoiling during DNA replication. *Int J Mol Sci* 2020;21:4504. <https://doi.org/10.3390/ijms21124504>
30. Ferrándiz MJ, Hernández P, de la Campa AG. Genome-wide proximity between RNA polymerase and DNA topoisomerase I supports transcription in *Streptococcus pneumoniae*. *PLoS Genet* 2021;17:e1009542. <https://doi.org/10.1371/journal.pgen.1009542>
31. Guo MS, Kawamura R, Littlehale ML *et al.* High-resolution, genome-wide mapping of positive supercoiling in chromosomes. *eLife* 2021;10:e67236. <https://doi.org/10.7554/eLife.67236>
32. Bates AD, Maxwell A. DNA gyrase can supercoil DNA circles as small as 174 base-pairs. *EMBO J* 1989;8:1861–6. <https://doi.org/10.1002/j.1460-2075.1989.tb03582.x>
33. Zhang Y, Cui Y, An R *et al.* Topologically constrained formation of stable Z-DNA from normal sequence under physiological conditions. *J Am Chem Soc* 2019;141:7758–64. <https://doi.org/10.1021/jacs.8b13855>
34. Li Q, Li J, Cui Y *et al.* Two-holder strategy for efficient and selective synthesis of Lk 1 ssDNA catenane. *Molecules* 2018;23:2270. <https://doi.org/10.3390/molecules23092270>
35. Thibault T, Degrouard J, Baril P *et al.* Production of DNA minicircles less than 250 base pairs through a novel concentrated DNA circularization assay enabling minicircle design with NF-κB inhibition activity. *Nucleic Acids Res* 2017;45:e26. <https://doi.org/10.1093/nar/gkw1034>
36. Du Q, Kotlyar A, Vologodskii A. Kinking the double helix by bending deformation. *Nucleic Acids Res* 2008;36:1120–8. <https://doi.org/10.1093/nar/gkm1125>
37. Sui Z, Liu M, Wang W *et al.* Efficient preparation of large-sized rings of single-stranded DNA through one-pot ligation of multiple fragments. *Chem Asian J* 2019;14:3251–4. <https://doi.org/10.1002/asia.201900963>
38. Hu K, Sun W, Tang R *et al.* Ethanolamine derivatives prompt oxidation-mediated cleavage of phosphorothioated DNA via redox control and competition with desulphurization. *Bull Chem Soc Jpn* 2022;95:1578–90. <https://doi.org/10.1246/bcsj.20220236>
39. Wang J, Pan X, Liang X. Assessment for melting temperature measurement of nucleic acid by HRM. *J Anal Methods Chem* 2016;2016:5318935. <https://doi.org/10.1155/2016/5318935>
40. Liang X, Kuhn H, Frank-Kamenetskii MD. Monitoring single-stranded DNA secondary structure formation by determining the topological state of DNA catenanes. *Biophys J* 2006;90:2877–89. <https://doi.org/10.1529/biophysj.105.074104>
41. Bucka A, Stasiak A. Construction and electrophoretic migration of single-stranded DNA knots and catenanes. *Nucleic Acids Res* 2002;30:24e–24. <https://doi.org/10.1093/nar/30.6.e24>
42. van den Broek B, Noom MC, Wuite GJL. DNA-tension dependence of restriction enzyme activity reveals mechanochemical properties of the reaction pathway. *Nucleic Acids Res* 95:2676–84.

43. Chen H, Gu Z, Yang L *et al.* Direct dsRNA preparation by promoter-free RCT and RNase H cleavage using one circular dsDNA template with a mismatched bubble. *RNA* 2023;29:1691–702. <https://doi.org/10.1261/rna.079670.123>
44. Stolz R, Sulthana S, Hartono SR *et al.* Interplay between DNA sequence and negative superhelicity drives R-loop structures. *Proc Natl Acad Sci USA* 2019;116:6260–9. <https://doi.org/10.1073/pnas.1819476116>
45. Chedin F, Benham CJ. Emerging roles for R-loop structures in the management of topological stress. *J Biol Chem* 2020;295:4684–95. <https://doi.org/10.1074/jbc.REV119.006364>